# L-lysine derived nickel nanoparticles for reductive degradation of organic dyes

Abdul Rauf Khaskheli[1,4*], Saba Naz[2,6], Razium Ali Soomro[3], Faruk Özel[4], Abdalaziz Aljabour[4], Nazar Hussain Kalwar[2], Abdul Waheed Mahesar[5], Imren Hatay Patir[4], Mustafa Ersoz[4,6]

[1]Department of Pharmacy, Shaheed Mohtarma Benazir Bhutto Medical University, Larkana, Sindh 77170, Pakistan
[2]Dr. M.A. Kazi Institute of Chemistry, University of Sindh, Jamshoro 76080, Pakistan
[3]Interface Analysis Centre, School of Physics, University of Bristol, Bristol, BS8 1TL, UK
[4]Karamanoğlu Mehmetbey University, Metallurgical and Materials Engineering Department, 70200 Karaman, Turkey
[5]Institute of Information and Communication Technology, University of Sindh, Jamshoro 76080, Pakistan
[6]Department of Chemistry, Faculty of Science, Selcuk University, Konya 42075, Turkey

[*]Corresponding author. Tel.: (+ 92) 33-32617777; Fax: (+92) 749410910;
E-mail: arkhaskheli@gmail.com, farukozell@gmail.com

## ABSTRACT

This report demonstrates a facile and green fabrication method for the nickel nanoparticles using L-lysine as an efficient protecting agent. The application of green amino acid (L-lysine) enabled formation highly spherical and well-dispersed nanoparticles with average diameter in the range of 10 ±2.5 nm. UV-Vis spectroscopy was used as a primary tool to elaborately study and optimize the necessary experimental condition for the developed synthetic protocol. Fourier transform infrared spectroscopy (FTIR) was used to confirm the surface protection of Ni NPs via L-lysine molecules whereas; atomic force microscopy (AFM) and scanning electron microscopy (SEM) provided morphological and topographical view of the as-synthesized Ni NPs. In addition, small angle X-ray scattering (SAXS) and X-ray diffraction (XRD) were used to evaluate compositional characteristics of fabricated L-lysine protected Ni NPs. The as-synthesized Ni NPs demonstrated excellent catalytic potential when utilized as heterogeneous catalyst for reduction of methylene Blue (MB) in the presence of sodium borohydride (NaBH$_4$). The observed catalytic reaction was determined to follow pseudo first order kinetics with rate constant (K) and turn over frequency (TOF) determined to be 0.0224 and TOF value of 0.00411 s$^{-1}$ respectively. Copyright © 2016 VBRI Press.

Keywords: Nickel nanoparticles; L-lysine; AFM; MFM; SEM; XRD; methylene blue.

## Introduction

The recent advancement in nanotechnology has led to development of highly efficient materials with diverse applications in multiple fields such optics, electronics and catalysis [1]. Metal nanoparticles, in this regards are most widely utilized and discussed materials because of their unique characteristics which are widely different from their bulk counterpart [2]. The nanoscale metals such as gold (Au), silver (Ag), nickel (Ni) and copper (Cu) are most widely studied materials with much interest propagating towards their catalytic potential when used as heterogeneous catalysis [3]. In particular, heterogeneous catalysis of environmental pollutants is of high concern due to the associated health and environmental contamination threat. The extensive usage of industrially important dyes, may lead to their accumulation in fresh water aquifers which may cause serious health related issues. Variety of approaches like, adsorption [7], biological discoloration [8] and advanced oxidation processes such as the photo-fenton reaction [9] and photo catalytic degradation by UV irradiation [10], visible light [11] and microwave discharge lamps [11, 12] are well regarded for the removal or degradation of dyes from wastewaters. Although, the presently utilized strategies for remediation of such colored

toxins are adequate but suffer the disadvantages like lengthy protocols, inefficient and incomplete removal of colored toxins [4-5]. Contrary to this, the reductive degradation of such colored dyes using highly efficient nano-size catalyst is a more rapid, simple and economic [13-14]. This strategy is not only viable in terms of efficiency and costliness but also greener as it provides biodegradable remains like aromatic amine, which are readily and easily degraded by microorganisms. Lang., *et al.* in 2008 used Pd nanoparticles with good catalytic properties in the degradation of azo dyes [15]. Similarly, nickel nanoparticles obtained by a wet chemical approach in an aqueous medium were employed for the complete degradation of Congo Red dye [16]. At present, from diverse variety of metals available, extensive interest has been observed towards the nickel metal nanoparticles due to its widespread and efficient application in numerous fields, for instance, microwave radiations absorbing substance, household batteries and diverse catalytic applications [17]. There are numerous reports over the synthesis and application of Ni NPs as catalyst. However, most of the utilized procedure for the synthesis of Nis NPs are either associated with usage of high energy or

requirement of especial equipment. In this regard, the usage of simple wet-chemical reduction method provides much greater privilege based on its simplicity, low-cost, rapid and choice of simple apparatus. In addition to this, the usage of various ligand molecules as effective protecting agents provides additional advantage of easy controlling dimension, shape, morphology of as-synthesized nanoparticles. In our previous study, Kalwar, N. H., *et al.* (2015) explored the catalytic capability of prepared Ni NPs for the reduction of pesticides. The report focused on the usage of L-serine as protecting agent and its role in producing well-dispersed and highly active Ni NPs for degradation of imidacloprid in aqueous solution [**6**]. Thus, keeping in mind the efficiency of amino acid as protecting agent and catalytic potential of Ni metal at nano scale dimension, this study explores the capability of L-lysine to function as efficient protecting agent for nickel nanoparticles. The as-synthesized Ni NPs were further studied for their catalytic potential when utilized for the reductive degradation of MB in aqueous environment in the presence of $NaBH_4$ reductant. The determined high reaction rate constant $(0.0224 \text{ s}^{-1})$ and turn over frequency (TOF) $(0.00411 \text{ s}^{-1})$ indicated the extreme catalytic potential of Ni NPs towards target dye. Moreover, the study signifying the non-poisonous characteristic of Ni NPs that can be easily recovered and reprocessed several times deprived of their activity reduction like fresh Ni NP. The synthesis protocol of Ni NP does not necessitate extended time preparation, energy or distinct apparatus which result in small sized, regular shapes and significantly narrower Ni NPs size distributions.

## Experimental

### Chemicals and reagents

The synthesis protocol of nanoparticle was conceded by means of analytical grade chemicals i.e. 97%, $NiCl_2.6H_2O$ (E. Merck), 99% L-lysine (Fluka), and other reagents like 98%, $NaBH_4$, 98% NaOH and 37% HCl (Sigma-Aldrich). For reaction medium ultrapure water was consumed in current study.

### Instrumentation

Fourier Transform Infrared (FTIR) results were attained by overlapping the spectra of L-lysine standard and L-lysine capped Ni NPs using a Vertex 70 (Bruker, Germany) with Platinum ATR Diamond. Atomic Force Microscopy (AFM) results were collected via NT-MDT, NTEGRA (Russia) AFM, MFM and Nanoscope IV controller. The morphological descriptions of Ni NPs were recorded through Scanning Electron Microscopy (SEM) EVO LS 10, AEISS (England), taken on Aluminum sample holder. Energy dispersive X-ray (Analysis) EDX, was completed with Bruker 123 eV (Germany). X-ray diffraction (XRD) pattern of dispersed NPs were collected using a Bruker Advance D8 XRD, Germany (Cu α source with 1.5406 wavelengths).

### The protocol of stock standard solutions

The standard concentration of L-lysine (0.1M), $NiCl_2.6H_2O$ (0.1M) and $NaBH_4$ (0.5M) were prepared. The required quantities of each standard concentration were poured in 100 mL volumetric flasks and added ultrapure water upto mark for the dilution purpose. To maintain the pH of each fresh solution of Ni NPs, acidic HCl (0.1M) and basic NaOH (0.1M) reagents were used respectively.

### The route for the synthesis of Ni NPs

In distinctive experiment, 0.02 mL (0.1 M) $NiCl_2.6H_2O$, 0.04 mL (0.1 M) L-lysine and 0.06 mL (0.5 M) $NaBH_4$ were mixed upto 10 mL sample by adding ultrapure water at room temperature. The appearance of mixed solution becomes black by the addition of reducing ($NaBH_4$). The pH of the solution was 9.5 without using any basic compound. To confirm the maximum reduction of nickel ions the mixed solution was allowed to left for 10-15min followed by the addition of capping agent to generate nano sized material.

### Nanoparticle separation

Water solvated L-lysine derived Ni NPs were isolated with the aid of rapid centrifugation process using a VWR Compact star CS 4 centrifuge, operated at 6000rpm for 3 minutes. The solid Ni NPs were settled down in the bottom and little stick on the walls of centrifugation tube, then dry with hot air and collected with 99% purity.

### FTIR study protocol

L-lysine capped Ni NPs were segregated from the disperse solution by placing large amount into petri dishes followed by drying at 80°C in automatic hot water bath. Furthermore, drying step was carried out at 100°C in an oven for at least 30min to ratify the complete evaporation of water molecules. Then dried material from petri dishes surface was collected by scraping the NPs and processes for FTIR study.

### AFM study protocol

In a typical AFM analysis 10-20µL of aqueous L-lysine derived Ni NPs were dispersed through drop casting method on glass cover slip and heated at 60°C for 30 min followed by air drying up to 5min to corroborate the glass surface binding of Ni NPs through evaporation of water moieties.

### SEM study protocol

Samples of dispersed L-lysine derived Ni NPs were mounted on aluminum sample holder in small quantities (Gold spuater quarter 7 nm), via method of dip coating. After that vacuum drying in a Cressington Sputter Coater, Auto 108, in the presence of Argon gas for 2min to clean the surface and to confirm the removal of solvent from surface.

### XRD study protocol

L-lysine derived solid state Ni NPs was isolated from dispersed solution by centrifuge the sample to get the products onto glass tube. Hot air was carried out for drying process until complete evaporation of the water. As

prepared L-lysine derived solid state Ni NPs were gathered by scraping the apparent nanoparticles from glass of centrifuge tubes and utilized for XRD analysis.

*Catalytic Potential of L-lysine capped Ni NPs*

The proficiency of newly synthesized Ni NPs in degrading the contaminants in aqueous medium was checked by using MB dye as model test contaminant. According to procedure, 3.5 mL of 100 μM MB dye with 10 mM $NaBH_4$ reductant solution present in a cuvette was treated with 0.1 mg of pure Ni NPs, previous adhered to a pre-weighted glass cover slip. The decrease in absorbance intensity signifying the deprivation of organic dye sat maximum absorbance of 650 nm and the data was further used for kinetic and catalytic parameters.

## Results and discussion

In the present experimental findings, we synthesized L-lysine derived Ni NPs with rough surface having fair size distributions. The proof of fabricated L-lysine derived Ni NPs was investigated through FTIR, AFM/MFM, SEM and XRD/SAXS analysis.

*FTIR study*

FTIR spectra for L-Lysine standard and L-lysine derived Ni NPs are presented in **Fig. 1**.
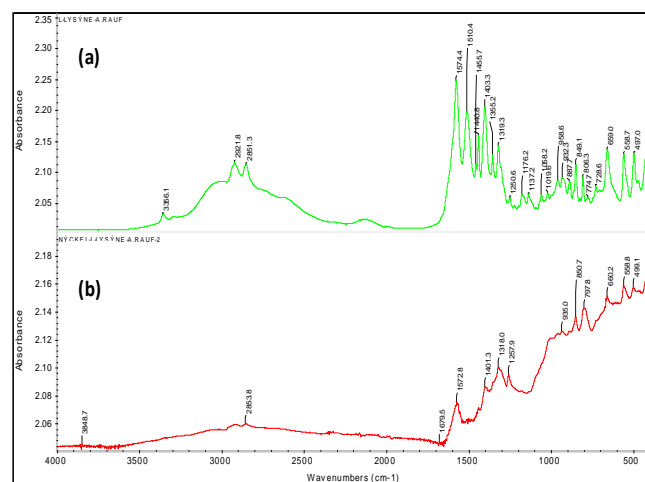


**Fig. 1.** (a) FTIR spectra for L-Lysine standard (b) L-lysine capped Ni NPs.

The above cited spectra offer supportive proof for nanoparticles production assessed by similar distributions which reveals through their UV-Vis studies and AFM images. **(Fig. 1(a))** illustrated a zwitterionic band in the standard L-lysine spectrum at 2164-2138cm⁻¹which is not present in Ni NPs spectrum **(Fig. 1(b))**. Two intense and broad signals appeared at 1572 cm⁻¹ and 1401 cm⁻¹ which allocated for hydroxyl groups [**21, 22**]. Analogous signals have been observed at 1651cm⁻¹ and 1382cm⁻¹ by other workers [**23**]. The spectral bands lower than 1500cm⁻¹ is allotted to bending vibrations of C-H due to methylene groups and the other IR weak band ranging from 1300-935 cm⁻¹ can be ascribed to stretching vibration of C-N owing to amino groups [**24**]. It is clarified from both standard L-lysine as well as L-lysine capped Ni-NPs

spectra in **Fig. 1** that, one broad band above 2851 cm⁻¹ is present with no changes corresponding to the existence of stretching frequencies of hydroxyl band at 2921 cm⁻¹ and amino band at 2853 cm⁻¹ experienced by -COOH and $-NH_2$ groups. This assures the chemical binding of Ni NPs via amino group linkage on the surface of capping agent.

*AFM study*

The formation of well distributed Ni NPs is shown through their AFM and MFM image scrapped with L-lysine molecules as represented in **Fig. 2(a,b)** respectively. Atomic force microscopy is effective and precise tool to quantitatively measure the particle size and dimensions in diverse surfaces, such as nanosized material adsorbed on different substrate surfaces.
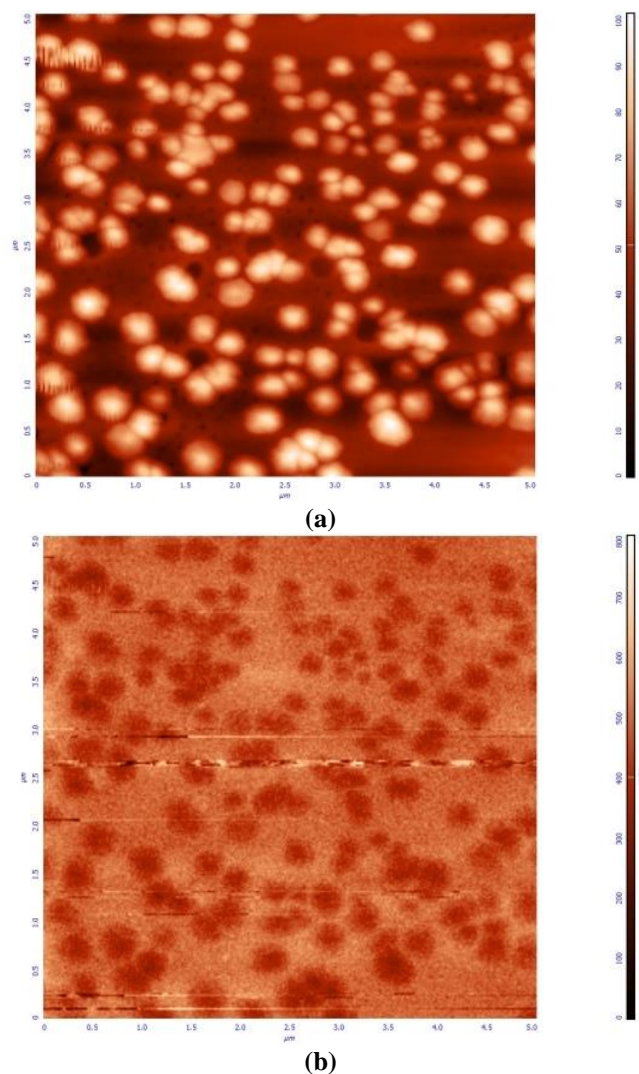


**(a)**



**(b)**

**Fig. 2.** (a) Typical medium scale AFM image of Ni NPs (0.5μm×0.5μm) (b) MFM images of L-Lysine capped Ni NPs (0.5μm×0.5μm).

The AFM images represent the color changes in Ni NPs solution, size dispersion, and systematic diagram of the creation of Ni NPs through precise interactions. AFM result exposed that the nickel particles products correspond to well dispersed and roughed surface. Every individual L-lysine molecule could possibly be attached on the small nanocomposites surface with similar shapes resulting

structure. The AFM and MFM results were in good agreement reveals through their similar nanoscale dimensions and size homogeneity.

*SEM study*

For the purpose of SEM imaging, Ni NPs were drop casted from aqueous solution and allow evaporating the water. The SEM micrographs represent the formation of different morphological structures with precisely ordered 2D nanospheres/foils geometry additionally; have smooth surface thickness ranging from10-100 nm. Conversely the average thickness is 20 nm. these nanospheres are found in 100-200nm in diameter, 60nm was calculated as an average diameter, and size of spherical Ni NPs ranging from 5-80 nm, with an observed 9 nm average size as presented in **Fig. 3(a,b)** corresponding to low and high resolution respectively. The presence of nickel was also confirmed by EDX using same samples of Ni NPs.
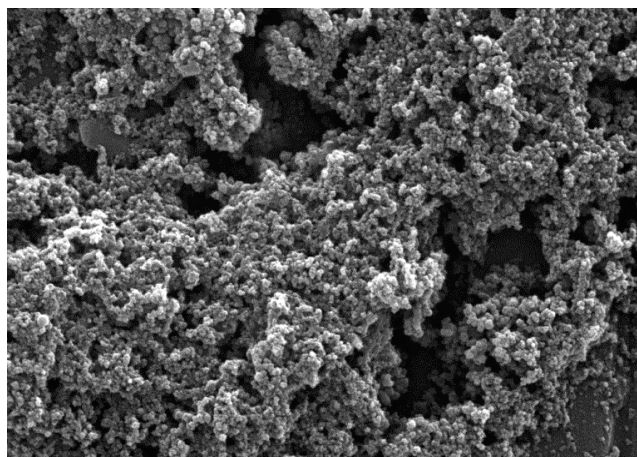


**(a)**
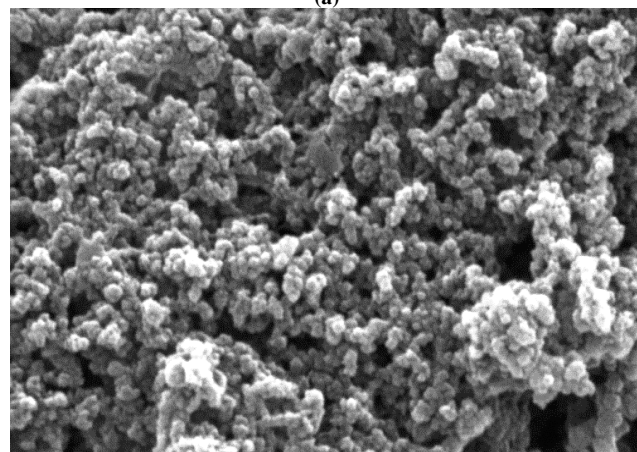


**(b)**

**Fig. 3.** (a) Low resolution (b) High resolution SEM micrographs of L-lysine capped Ni NPs.

*XRD study*

The crystal structure and phase composition of the L-lysine derived Ni NPs were carried out by powdered XRD analysis as depicted in **Fig. 4**. The XRD pattern shows that L-lysine protected Ni NPs. The XRD peaks of nano-sized nickel showed characteristic peaks with 2θ values of

34.45°, 44.48°, 60.27° and 71.02° indexed to (110), (111), (200) and (220) crystal planes of FCC structures [**25**]. The crystallite size was estimated by using Sherrer's formula over the intense peak indexed to (200) plane of Ni. The estimated crystallite size of 8 nm is consistent with size determined (7 nm) using SAXS analysis shown in **Fig. 4(b)**.
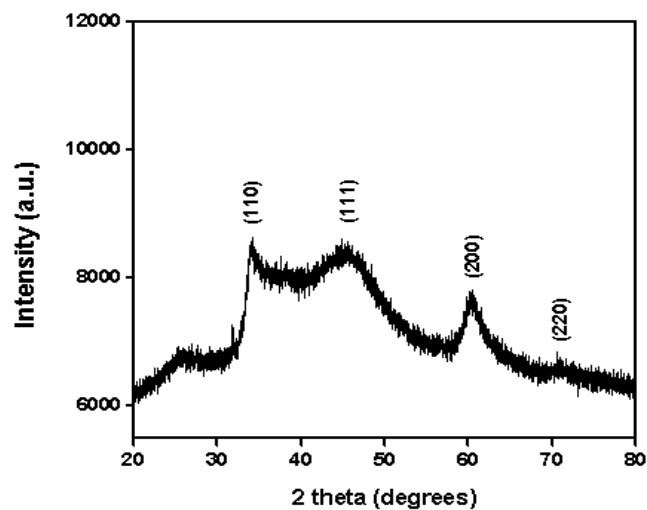


**(a)**
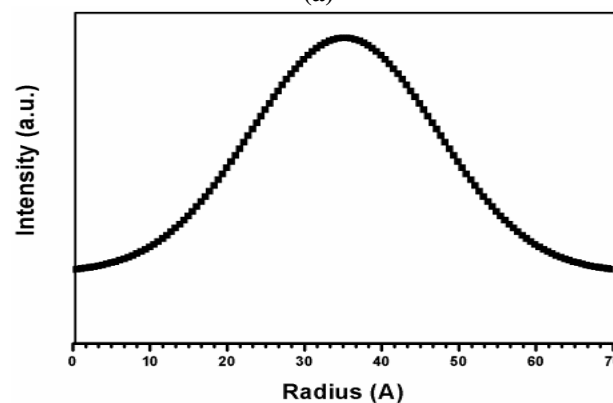


**(b)**

**Fig. 4.** (a) XRD pattern (b) SAXS plot for L-Lysine stabalized Ni NPs.

*The catalytic evaluation of the as-synthesized Ni NPs*

The catalytic performance of synthesized Ni NPs was observed by using UV-vis spectroscopy. The MB dye was used as a standard pollutant as it is broadly used as an indicator for the estimation of catalytic activity of nanoparticles. The degradation of MB can be easily observed using UV-vis spectroscopy owing to its absorption peak in the visible region at 650 nm [**31**]. The un-catalyzed reaction was carried to evaluate the capability of reducing agent along with dye. The reaction was performed with NaBH$_4$ (10mM) with MB (100μM), which showed only small percentage of degradation (up to 8.5%) after the expense of 20 min time as shown in **Fig. 5(a)**. In contrast catalyzed reaction carried with Ni NPs in a similar sample environment showed complete (100%) degradation of MB (100 μM) just within 160 s of reaction time. It was also observed that the reaction rate of MB degradation with Ni NPs was enhanced 7.5 times with 100% degradation efficiency when compared with results

of the un-catalyzed reaction **Fig. 5(b)**. The data was found to follow first order kinetics given by equation 1; with rate constant of 0.0224 sec$^{-1}$ as depicted in **Fig. 5(c)**.
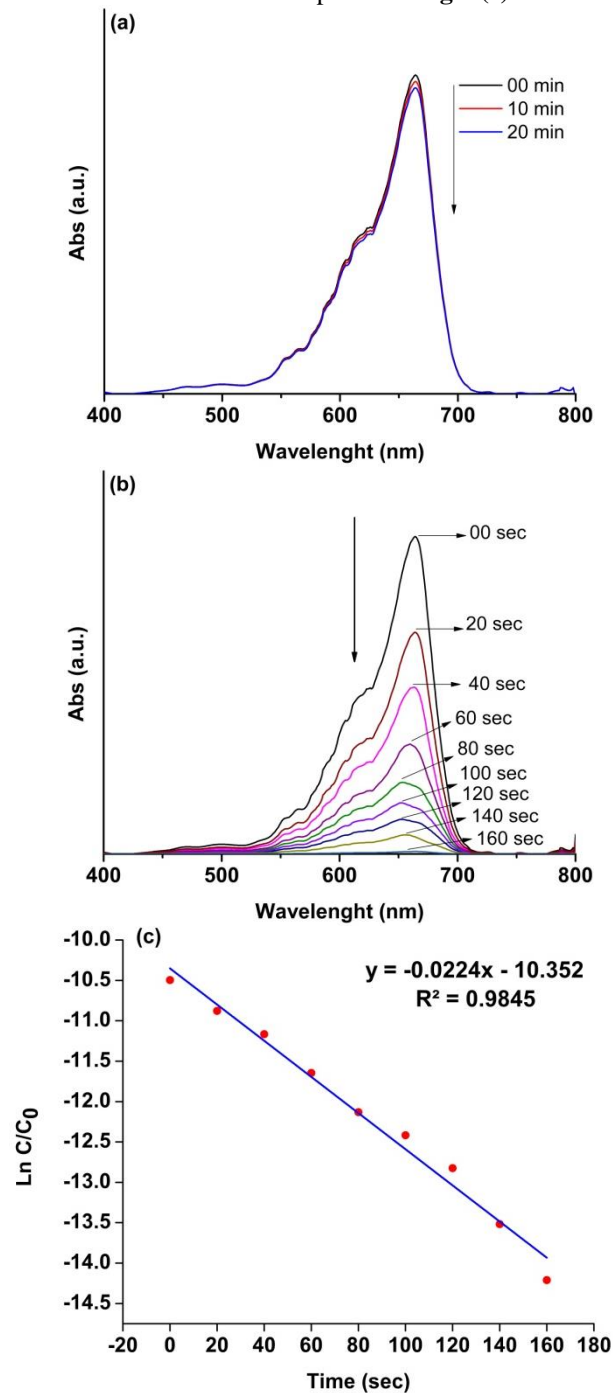


**Fig. 5.** UV-vis spectral analysis for catalytic reductive degradation of a MB: (a) Un-catalyzed reaction carried alone with 100 μM NaBH$_4$ (b) Catalyzed reaction carried with 100 μM NaBH$_4$ in the presence of a 0.1 mg of Ni NPs (c) Linear regression plot showing pseudo-first order kinetics for the catalyzed reductive degradation of MB with Ni NPs.

$$\ln \frac{C}{C_o} = -kt \qquad (1)$$

$$TOF = \frac{-k_1\left(s^{-1}\right) \times \left[Analyte\right]_{t=0}(M)}{\left[NiNPs\right](M)} \qquad (2)$$

The turn over frequency (TOF) number was also calculated to evaluate the efficiency of catalyst (*i.e.* provided in equation 2); the TOF of the said reaction was found to be 0.00411 sec$^{-1}$.
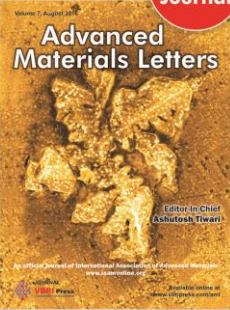
## Conclusion

In conclusion, the study explores the potential capability of L-lysine amino acid to function as effective protecting agent for nickel nanoparticles. The elaborate characterization study indicated formation of highly dispersed, homogenous spherical nanoparticles with average diameter of 10 ±2.5 nm. The as-synthesized Ni NPs demonstrated excellent catalytic potential against reductive degradation of MB dye in aqueous solution owing to their high surface to volume ratio and rough surface architectures. The determined rate constant (K) 0.0224 s$^{-1}$ and TOF values 0.00411 s$^{-1}$ further numerically justifies the high surface catalytic capability of Ni NPs.

**Reference**

1. Naz, S.; Khaskheli, A.R.; Aljabour, A.; Kara, H.; Talpur, F.N.; Sherazi, S.T.H.; Khaskheli, A.A; and Jawaid, S., *Advances in Chemistry*, **2014**.
   **DOI:** org/10.1155/2014/686925.
2. Kumar, A.; Saxena, A.; De, A.; Shankar, R.; Mozumdar, S. *Adv. Nat. Sci.: Nanosci. Nanotechnol*, **2013**, *4*, 025009.
   **DOI:** 10.1088/2043-6262/4/2/025009.
3. Bothra, S.; Solanki, J. N.; Sahoo, S. K. *Sensor Actuat B: Chem*, **2013**, *188*, 937-943.
   **DOI:** 10.1016/j.snb.2013.07.111
4. Wilson, C.; Tisdell, C. *Ecological economics* **2001**, 39, 449.
   **DOI:** 10.1016/S0921-8009(01)00238-5
5. Xu, L.; Wu, X.-C.; Zhu, J.-J. *Nanotechnology* **2008**, *19*, 305603.
   **DOI:** 10.1088/0957-4484/19/30/305603
6. Kalwar, N. H.; Nafady, A.; Sherazi, S. T. H.; Soomro, R. A.; Hallam, K. R.; Khaskheli, A. R.; Jamali, A. A. *Materials Express* **2015**, *5*, 121.
   **DOI:** http://dx.doi.org/10.1166/mex.2015.1224.
7. Gezici, O.; Kucukosmanoglu, M.; Ayar, A.; *J. Colloid. Interf. Sci*, **2006**, 304,307.
   **DOI:** 10.1016/j.jcis.2006.09.048
8. Jones, J.J.; Falkinham, J.O.; *Antimicrob. agents chemother*, **2003,** 47, 2323.
   **DOI:** 10.1128/AAC.47.7.2323-2326.2003
9. Alshamsi, F.A.; Albadwawi, A.S.; Alnuaimi, M.A.; Rauf, M.A.; Ashraf, S.S.; *Dyespigments,* **2007**, 74, 283.
   **DOI:** 10.1016/j.dyepig.2006.02.016.
10. Saquib, M.; Muneer, M.; *Dyes pigments*, **2003**, 56, 37.
    **DOI:** 10.1016/S0143-7208(02)00101-8.
11. Hong, J.; Sun, C.; Yang, S.G.; Liu, Y.Z.; *J. Hazard. Mater,* **2006,** 133, 162.
    **DOI:** 10.1016/j.jhazmat.2005.10.004
12. He, Z.; Sun, C.; Yang, S.G.; Ding, Y.C.; He, H.; Wang, Z. L.; *J. Hazard. Mater,* **2009**, 162, 1477.
    **DOI:** 10.1016/j.jhazmat.2008.06.047.
13. Ju, Y.M.; Yang, S.G.; Ding, Y.C.; Sun, C.; Zhang, A.Q.; Wang, L.H.; J. *Phys. Chem. A,* **2008**, 11, 11172.
    **DOI:** 10.1021/jp804439z
14. Chen, C.C.; Liao, H.J.; Cheng, C.Y.; Yen, C.Y.; Chung, Y.C.; *Biotechnol. Lett,* **2007,** 29, 391.
    **DOI:** 10.1007/s10529-006-9265-6
15. Lang, X.; Xing-Cai, W.; Jun-Jie, Z.; *Nanotechnol,* **2008**, 19, 305603.
    **DOI:** 10.1088/0957-4484/19/30/305603.
16. Ghosh, S.K.; Pal, T.; *Chem. Rev,***2007**,107,4797.
    **DOI:** 10.1021/ Cr0680282
17. Yu, C.; Yu, Y.; Sun, H.; Xu, T.; Li, X.; Li, W.; *Mater Lett*, **2007,** 61, 1859.
    **DOI:** 10.1016/j.matlet.2006.07.162
18. Faramarzi, A.; Sanjabi, S.; *J. Phys. Chem. C*, **2011**,115, 18958.
    **DOI:** 10.1021/jp204458f
19. Boudjahem, A. G.; Monteverdi, S.; Mercy, M.; Bettahar, M. M.; *J. Catal*, **2004,** 221, 325.

      **DOI:** 10.1023/B:CATL.0000038581.80872.7b

20. Laaksonen, P.; Kivioja, J.; Paananen, A.; Kainlauri, M.; Kontturi, K.; Ahopelto, J.; Linder, M. B.; *Langmuir,* **2009,** 25, 5185.
      **DOI:** 10.1021/la804001e

21. Gao, X. Y.; Wang, S. Y.; Li, J.; Zheng, Y. X.; Zhang, R. J.; Zhou, P.; Yang, Y. M.; Chen, L. Y.; *Thin Solid Films,* **2004**, 438, 455.
      **DOI:** 10.1016/j.tsf.2003.11.242.

22. Janardhanan, R.; Karuppaiah, M.; Hebalkar, N.; Rao, T. N.; *Polyhedron,* **2009**, 28, 2522.
      **DOI:** 10.1016/j.poly.2009.05.038.

23. Singla, M. L.; Negi, A.; Mahajan, V.; Singh, K. C.; Jain, D. V. S.; *Appl. Catal. A.***2007**,323,51.
      **DOI:** 10.1016/j.apcata.2007.01.047

24. Lei, Y.; Chim, W.; Zhang, Z.; Zhou, T.; Zhang, L.; Meng, G.; Phillipp, F.; *Chem. Phys. Lett,***2003,** 380, 313.
      **DOI:** 10.1016/j.cplett.2003.09.025

25. Wang, A.; Yin, H.; Lu, H.; Xue, J.; Ren, M.; Jiang, T.; *Langmuir,***2009,** 21, 12736.
      **DOI:** 10.1021/la901815b.